01 Jan 2024

DNA Origami-Assisted Regioselective Organization of Anisotropic Gold Nanotriangle Clusters

Wenyan Liu
Missouri University of Science and Technology, liuweny@mst.edu

Prashant Gupta

Yuwei Zhang

Krishna Thapa

et. al. For a complete list of authors, see https://scholarsmine.mst.edu/chem_facwork/4024

Recommended Citation

W. Liu et al., "DNA Origami-Assisted Regioselective Organization of Anisotropic Gold Nanotriangle Clusters," *ACS Applied Optical Materials*, American Chemical Society, Jan 2024.
The definitive version is available at https://doi.org/10.1021/acsaom.4c00086

ACS APPLIED OPTICAL MATERIALS

Editors' Choice

pubs.acs.org/acsaom

Forum Article

DNA Origami-Assisted Regioselective Organization of Anisotropic Gold Nanotriangle Clusters

Wenyan Liu, Prashant Gupta, Yuwei Zhang, Krishna Thapa, Srikanth Singamaneni, and Risheng Wang*

Cite This: https://doi.org/10.1021/acsaom.4c00086

Read Online

ACCESS | Metrics & More | Article Recommendations | Supporting Information

ABSTRACT: The manipulation of anisotropic nanoparticles, such as gold nanorods and nanoprisms, has attracted great attention in nanotechnology due to their sensitive geometry-dependent properties. However. traditional synthesis and assembly methods for these particles face challenges in size uniformity and higher-order structuring. To address these limitations, this study presents a strategy using DNA origami triangles, not just as templates, but as encapsulating agents for gold nanotriangles (AuNTs). This method enables the construction of diverse nanoparticle clusters with precisely controlled distance and orientation. The formed clusters exhibit unique optical characteristics, demonstrated by UV−visible spectroscopy and supported by finite-difference time domain (FDTD) simulations. The observed shifts in plasmon resonance peaks indicate significant electromagnetic interaction by organizing nanoparticles in proximity and show the potential of this method for creating highly sensitive biosensors and other nanophotonic applications.

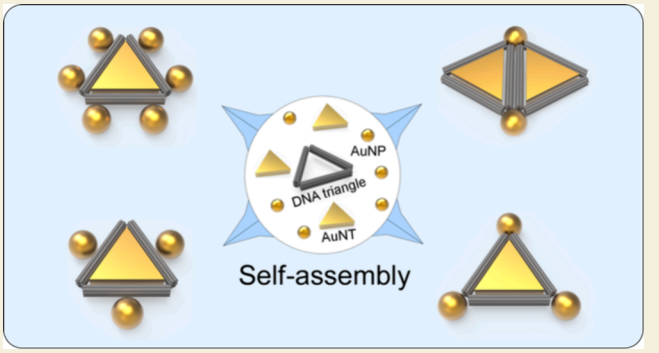

KEYWORDS: *Gold nanotriangle, DNA origami, Self-assembly, FDTD simulation, Gold nanoparticles, Plasmonic resonance*

INTRODUCTION

Anisotropic nanoparticles, particularly gold nanostructures like nanorods and nanoprisms, are studied extensively due to their geometry-sensitive and tunable physical and optical properties.[1−6] The synthesis process, which employs various methods to yield nanoparticles with uniform sizes and exceptional properties, remains complex and challenging.[7−12] The assembly of higher-order structures and heteroclusters is particularly difficult due to shape restrictions that often result in one-dimensional stacking columns or closely packed two-dimensional arrays.[13−20] Recent decades have seen the use of lithography techniques to pattern nanotriangles, but these approaches have limitations, including time-consuming and costly, as well as lack of assembly diversity.[21−24] In contrast, bottom-up self-assembly methods, such as polymer and DNA-assisted formation of laminar structures, have been explored.[25−28] However, these too have been hindered because it typically resulted in structures with limited diversity.

To overcome these limitations, novel functionalization methods have been introduced to improve directional control during nanotriangle assembly, including the strategic regioselective surface encoding of nanoparticles using diblock copolymers.[29] This approach has yielded various complex nanoparticle assemblies. A particularly notable advance was made by Ding et al., who utilized DNA origami as a template to align two gold nanotriangles into a bowtie motif with gaps as small as 5 nm, creating highly sensitive biosensors.[30] Motivated by the versatility and precise programmability offered by DNA origami,[27,31] our work introduces a pioneering strategy to harness DNA origami triangles, not only as a scaffold but as an encapsulating agent for gold nanotriangles (AuNTs). This approach enables strategic organization with other gold nanoparticles (AuNPs) to construct diverse nanoparticle clusters, providing unprecedented control over their position and orientation. This precise manipulation enhances the optical properties of the nanoparticles, crucial for the development of plasmonic devices. The localized surface plasmon resonances (LSPRs) of AuNTs can be finely tuned by adjusting their arrangement and proximity, facilitating the development of highly sensitive sensors. For instance, assembled AuNTs can be used in the fabrication of plasmonic sensors that detect chemical or biological substances at extremely low concentrations.[32] By leveraging the enhanced electromagnetic fields generated at the edges and corners of these triangles, such sensors can achieve superior sensitivity compared to traditional plasmonic devices. The optical characteristics of these nanoparticle clusters are confirmed by

Special Issue: Optical Applications of DNA Nanotechnology

Received: February 21, 2024
Revised: June 13, 2024
Accepted: June 14, 2024

UV−vis spectroscopy and corroborated by finite-difference time domain (FDTD) simulations, highlighting significant advancements in the field of nanotechnology. This work not only allows for the spatial manipulation of nanoparticles at the nanometer scale but also opens up possibilities for new optical phenomena and a wider range of nanoscale technological applications.

EXPERIMENTAL SECTION

Materials

All chemicals were obtained from Fisher Scientific and used as received. All chemically synthesized DNA strands were purchased from Integrated DNA Technologies, Inc. (www.Idtdna.com). The unmodified staple strands were ordered in a 96-well plate format, suspended in ultrapure water without purification. M13mp18 DNA scaffold was purchased from Bayou Biolabs. AuNPs were purchased from Ted Pella, Inc.

Preparation of DNA Origami

DNA origami triangle was designed using caDNAno. For the origami sample preparation, M13mp18 viral DNA and staple strands were mixed at a ratio of 1:5 in 1 × TAE buffer solution containing 40 mM Tris-HCl, 20 mM acetic acid, 2 mM of EDTA, and 11.5 mM magnesium acetate. The assembly was facilitated according to the following program: 90 °C for 10 min, 85 to 65 °C for 1 h, then slowly cooling from 65 to 15 °C over 12 h using a thermal cycler, resulting in a final M13mp18 DNA concentration of 20 nM.

Synthesis of Gold Nanotriangles

Gold nanotriangles were synthesized by adapting a method from existing literature.[17] Initially, 48 mL of 0.1 M CTAC was diluted in 336 mL of Milli-Q water, followed by the addition of 3 mL of 10 mM KI, stirred at 350 rpm for 3 min. Subsequently, 3.2 mL of 25.4 mM $HAuCl_4$ and 0.8 mL of 0.1 M NaOH were introduced to yield a pale-yellow solution. The reduction reaction was triggered by adding 4 mL of 64 mM ascorbic acid while stirring at 350 rpm for 30 s, and then 800 μL of 0.1 M NaOH was added with a quick shake for 3 s. The solution was left undisturbed at room temperature for 2 h, after which the AuNTs were isolated by centrifugation at 4200 RCF for 10 min and resuspended in water. A crucial step in ensuring successful synthesis was thoroughly cleaning the reaction vessels with aqua regia and distilled water to eliminate contaminants.

Preparation of DNA-Functionalized Gold Nanoparticles and Gold Nanotriangles

Thiolated DNA was anchored to gold nanoparticles through a functionalization process. SH-DNA strands were activated with TCEP at room temperature for 1 h and subsequently purified via a G-25 column. These freshly prepared oligonucleotides were then introduced to the AuNP solutions in an 800:1 molar ratio. SDS at 0.01% concentration was included for nanoparticle solutions. The binding was allowed to proceed at room temperature for 1 h. In the salting process, The NaCl concentration of the mixture was gradually increased to 50 mM by using a syringe infusion pump adding 2 M NaCl with speed of 4 μL/min. Postincubation, the nanoparticles were centrifuged to discard excess DNA, resuspended in PBS buffer with 25 mM NaCl, and washed thrice. The final gold nanoparticle dispersion in PBS was characterized using UV−vis spectroscopy. The sequences of thiol-DNA used to functionalize AuNTs and AuNPs are HS-AuNTP-10HB: /5ThioMC6-D/TTTTTTTTTTCTTCGTAGTG and HS-AuNP-10HB: /5ThioMC6-D/TTTTTTTTTTGATT-GACAGC, respectively.

Preparation of DNA Origami-Assisted AuNT-AuNP Clusters

Origami structures were combined with AuNTs and AuNPs at a 1:3:9 molar ratio for the cluster with three AuNPs, 1:3:20 for the clusters with six AuNPs, and 1:3:8 molar ratio for the dimers, in 1xTAE buffer with 11.5 mM magnesium acetate. This mixture was annealed from 50 °C down to 30 °C over 12 h. Following annealing, the clusters were isolated by agarose gel electrophoresis and the relevant bands were excised for TEM analysis and UV−vis characterization.

Agarose Gel Electrophoresis

For the agarose gel, the samples were loaded into 0.8% agarose gel that contained 5 mM $Mg(CH_3COO)_2$ in a 1 × TAE buffer solution under 55 V at room temperature. The gel was stained with ethidium bromide for visualization.

AFM Imaging

The AFM images were obtained using the Bruker Dimension Icon instrument. Three μL of DNA origami sample was applied onto freshly cleaved muscovite mica (Ted Pella, Inc.) for 60 s. After the fixation of the targeted structure of DNA origami on the mica surface, double-distilled H_2O (50 μL) was dropped on the mica to remove the buffer salts, then the drop was wicked off, and the sample was dried with compressed air. Imaging was performed in ScanAsyst mode using ultrasharp 14 series (NSC 14) tips from NANOANDMORE.

TEM Imaging

For TEM, a 5 μL sample was applied to a carbon-coated grid and left to absorb for 3 min. Excess solution was wicked away, and the grid was stained with 2% uranyl acetate for 15 s before drying at room temperature. Imaging was conducted using a Tecnai F20 instrument.

Finite-Difference Time-Domain (FDTD) Simulations

Commercially available three-dimensional finite-difference time-domain (FDTD) simulations software (EM Explorer) was employed to reveal the Electromagnetic field distribution around various nanoparticle clusters. In FDTD simulations, the time and space dependence of maxwell's equations is employed to map the electromagnetic waves in a finite volume rectangular 3D cells called "Yee cells".[33] Perfectly matched layer (PML) absorbing boundary conditions were imposed in all directions of the simulation domain. The AuNT core was defined as an equilateral triangle of edge length of 48 nm and thickness of 20 nm. The AuNPs were defined as a sphere with a diameter of 33 nm and the interparticle distances for the nanoparticle clusters were defined as depicted in Figure S1. The dimensions of AuNT, AuNP and interparticle distances were measured using the TEM micrographs and the thickness of AuNT was measured using AFM. The simulation domain was defined to be 200 nm x 200 nm x 100 nm. To obtain simulated extinction spectra of the developed nanoparticle clusters, a high-resolution simulation (Yee cell size of 1 nm) was run at excitation wavelengths ranging from 400 to 800 nm at 10 nm interval utilizing p-polarized incident plane wave illumination. The wavelength dependent complex refractive index of gold was employed and the refractive index of the surrounding medium was set to be 1 (that of air).[34] The electromagnetic field distribution was visualized by running a high-resolution simulation (Yee cell size of 1 nm) at the excitation (λ = 560 nm, peak position obtained from the simulated extinction spectra) utilizing p-polarized incident plane wave illumination to generate the electromagnetic field distribution. The complex refractive index was set to $n = 0.317 + i$ 2.837 for gold and the refractive index of the surrounding medium was set to be 1 (that of air).[33]

RESULTS AND DISCUSSION

The project starts with the engineering of a DNA origami scaffold shaped into an equilateral triangle with an edge length of ∼70 nm. The cross-section of this structure is assembled from a pair of intertwined six-helix bundles, as described in Figure 1A. The morphological fidelity of the origami triangle is confirmed by atomic force microscopy (AFM), which is consistent with the theoretical design (Figure 1B). Leveraging the versatile modification potential of DNA origami, DNA sticky ends are strategically selected to protrude from the internal and external edges, as well as the apexes of the DNA triangle. These functional sticky ends are used for the deterministic positioning of AuNTs and AuNPs, thus enabling

https://doi.org/10.1021/acsaom.4c00086
ACS Appl. Opt. Mater. XXXX, XXX, XXX−XXX

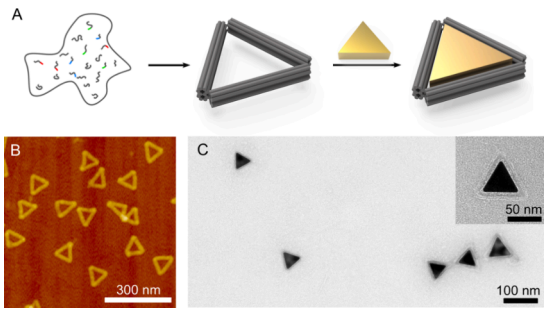

Figure 1. Assembly and characterization of DNA origami nanotriangles. (A) Depiction of the synthesis process for DNA origami nanotriangles and the subsequent encapsulation of gold nanotriangle (AuNTs). (B) Atomic force microscopy (AFM) image illustrating the successful formation of an equilateral nanotriangle with an approximate edge length of 70 nm. (C) Transmission electron microscopy (TEM) image demonstrating the central encapsulation of AuNTs within the DNA origami triangle structure.

the assembly of structurally diverse complexes. The detailed numbers of sticky ends and their locations on DNA origami used to assemble various nanoparticle clusters are shown in Figure S2. By following the surface functionalization of nanoparticle method,[27] thiol-modified single-stranded DNA (thiol-ssDNA) was conjugated to the surfaces of AuNTs and AuNPs, enabling hybridization with the complementary DNA sticky ends extending from the DNA origami scaffold. This hybridization is pivotal for guiding the assembly of the particles, as shown in Figure 2A. Transmission electron microscopy (TEM) imaging reveals the DNA origami encapsulated gold nanotriangles (Figure 1C). Contrasted against the chemically synthesized AuNTs (Figure S3), DNA origami-encapsulated nanotriangles demonstrate superior dispersion and size homogeneity. These characteristics are essential for the subsequent hierarchical assembly and the comprehensive characterization of their optical properties.

The innovative application of DNA origami-assisted assembly has enabled the creation of a series of intricate nanoparticle clusters, showcasing the technique's capacity for precision and versatility. By programming the sticky ends of DNA strands to extend from predetermined vertices and edges, a diverse array of nanoparticle arrangements was achieved. For example, when sticky ends were designed to protrude from the vertices of the DNA origami structure (Figure S2), clusters were formed with three AuNPs precisely situated at these vertices (Figure 2B). Altering the DNA design, AuNPs were also accurately positioned at the midpoints of the edges (Figure 2C). Moreover, by adjusting the spatial configuration, a total of six nanoparticles were precisely placed near the vertices to create a denser cluster (Figure 2D). In another configuration, AuNTs were aligned side by side with two AuNPs nestled centrally between them (Figure 2E). This assortment of configurations is captured in the TEM images, which confirm the well-defined formation of these clusters. Additional TEM images at a larger scale are presented in Figure S4. The TEM images present visual evidence of the clusters' precise geometric arrangements and the consistency in particle size and spacing, underscoring the successful application of DNA origami techniques. Further extending these findings, two additional cluster designs are presented in the Supporting Information (Figure S5). The self-assembly yield of each cluster, calculated based on agarose gel electrophoresis, varies from 31% to 42% as shown in Figure S6. These results not only confirm the structural fidelity of the clusters but also illuminate the potential of DNA nanostructures to enhance the self-assembly of complex, higher order nanoarchitectures.

The proximity of nanoparticles can indeed induce significant changes in their optical properties, a phenomenon that is one of the primary aims of nanoscale manipulation. Upon examination of the UV−vis absorbance spectra (Figure 3), distinct shifts in the plasmon resonance peaks were observed as a result of nanoparticle clustering. For isolated AuNPs, a pronounced absorption peak occurs at 530 nm, typically associated with the surface plasmon resonance of spherical nanoparticles. Similarly, the AuNTs exhibit a characteristic peak at 625 nm. However, when these nanoparticles are assembled into clusters, their interaction leads to a modification of their optical properties. Specifically, the spectrum of the nanospheres shows a red shift, indicating a change toward longer wavelengths. Conversely, the nanotriangles experience a blue shift, which corresponds to a move toward shorter wavelengths. This spectral behavior is illustrated in the provided graph, where the progressive red shift for nanospheres and blue shift for nanotriangles can be visualized as a function of cluster formation. The observed shift in peak wavelength is also associated with the assembly ratio between particles and the proximity of neighboring particles. In

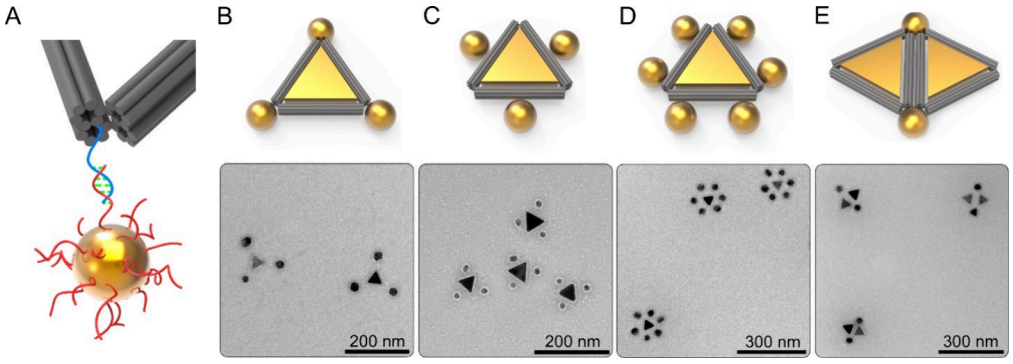

Figure 2. Precise assembly of nanoparticle clusters via DNA origami. (A) Diagrammatic illustration of the hybridization interaction between nanoparticles and DNA origami to form structured clusters. Configurations include three gold nanoparticles (AuNPs) at the triangle's vertices (B), AuNPs at the center of the edges (C), a hexagonal arrangement of six AuNPs (D), and a side-by-side alignment of AuNTs with two central AuNPs (E). The lower panels display TEM images confirming the specified nanoparticle formations.

https://doi.org/10.1021/acsaom.4c00086
ACS Appl. Opt. Mater. XXXX, XXX, XXX−XXX

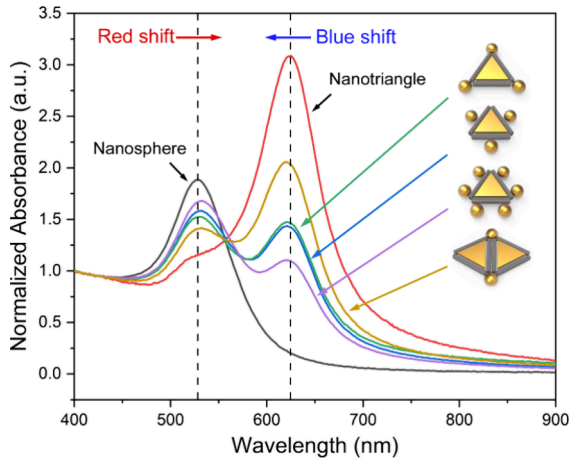

Figure 3. UV−visible absorbance spectra of gold nanoparticles and their clusters. This graph shows the change in light absorption when AuNPs and AuNTs are combined into clusters. The individual AuNP peak at 530 nm shifts to longer wavelengths (red shift), and the AuNT peak at 625 nm moves to shorter wavelengths (blue shift) upon clustering. The inset diagrams correspond to the different clustered structures studied."

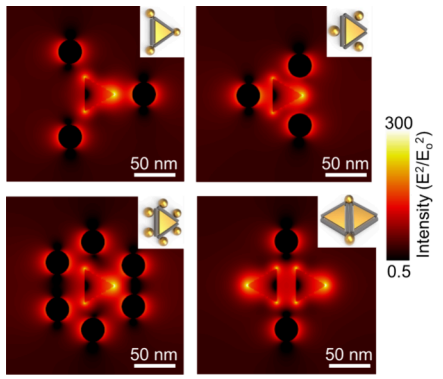

Figure 4. Finite-difference time-domain (FDTD) simulations illustrating the electromagnetic field intensity distribution around precisely assembled nanoparticle clusters via DNA origami. The insets show the different nanoparticle configurations investigated.

comparation, the mixtures of DNA origami with AuNPs and AuNTs in the absence of templated assembly were examined. The mixing these components results in a very subtle peak shift accompanied by peak broadening, suggesting slight particle aggregation occurs without the support of a template (Figure S7). The ability to manipulate the optical properties through the strategic combination of clusters highlights the precision and tunability of nanoparticle assembly via DNA origami techniques.

Precise tuning of localized surface plasmon resonance of metal nanoparticles is of paramount importance for their application in diverse fields including sensing, biomedicine, optoelectronic devices, catalysis and light- and energy-harvesting.[35] Owing to the fact that plasmon resonance endows these metal nanoparticle assemblies with extraordinary properties by creating plasmonic nanoantenna as a result of subwavelength localization of the electromagnetic field upon interaction with light.[36,37] We performed FDTD simulations to reveal the electromagnetic field intensity distribution around these precisely assembled nanoparticle clusters to further shed light on their optical properties. Based on the optical constants of gold, we employed FDTD simulations to calculate the extinction spectra of these metal nanoparticle assemblies (Figure S8).[38] The simulated extinction spectra (Figure S8) exhibited excellent agreement with the experimentally measured extinction spectra (Figure 3) of nanoparticle assemblies. The simulated spectra exhibited blue shift in the AuNT peak upon clustering, however the red shift in the AuNP peak was not obvious. The spatial maps of the electric filed intensity were calculated via FDTD simulation at plasmon resonance peak (λ = 560 nm, as observed from the simulated extinction spectra) to real the electromagnetic field intensity distribution around metal nanoparticle assemblies (Figure 4). As observed from the spatial maps, the electromagnetic filed intensity distribution is highly sensitive to the precise location of nanostructures in the clusters. These results systematically demonstrate the superiority of the demonstrated DNA origami technique in developing precisely tuned higher order plasmonic heterostructures and opens novel avenues in wide area of applications pertaining to plasmonic assemblies.[39]

CONCLUSION

In summary, the study presents a great advancement in the assembly of anisotropic nanoparticles, particularly AuNTs, using DNA origami techniques. The engineering of DNA origami scaffolds into precise geometric configurations has enabled the encapsulation and strategic organization of AuNTs into various complex clusters with extraordinary control over their spatial arrangement, which has been validated through AFM and TEM imaging. The optical properties of the assembled clusters were characterized by UV−visible spectroscopy, revealing pronounced plasmonic resonance shifts that consistent with the FDTD simulations. These shifts are indicative of the altered electromagnetic environment due to the proximity and precise arrangement of the nanoparticles. The red and blue shifts observed in the absorption spectra highlight the tunability of the clusters' optical behavior, which can be attributed to the collective interactions within the nanoparticle assemblies. Our innovative approach has demonstrated the potential to manipulate the electromagnetic field at the nanoscale, thereby enhancing the localized surface plasmon resonance. The successful implementation of DNA origami-assisted assembly introduces a versatile, cost-effective, and scalable method to create highly ordered, functional nanostructures. The findings of this research not only pave the way for the development of next-generation nanophotonic devices but also offer significant advancements in solar cell applications. By harnessing the collective plasmonic modes supported by arrays of AuNTs, we can improve light absorption and increase photovoltaic efficiency. The ability to control the spatial arrangement of AuNTs optimizes light trapping and scattering, thereby enhancing overall energy conversion efficiency.[40] Additionally, this foundational technique broadens the application of nanotechnology across various scientific and industrial fields.

ASSOCIATED CONTENT

Supporting Information

The Supporting Information is available free of charge at https://pubs.acs.org/doi/10.1021/acsaom.4c00086.

https://doi.org/10.1021/acsaom.4c00086
ACS Appl. Opt. Mater. XXXX, XXX, XXX−XXX

TEM image of chemical synthesized gold nanotriangles, precise assembly of nanoparticle clusters via DNA origami, FDTD simulation, and DNA sequences (PDF)

AUTHOR INFORMATION

Corresponding Author

Risheng Wang − *Chemistry Department, Missouri University of Science and Technology, Rolla, Missouri 65409, United States;* orcid.org/0000-0001-6539-1565; Email: wangri@mst.edu

Authors

Wenyan Liu − *Chemistry Department, Missouri University of Science and Technology, Rolla, Missouri 65409, United States*

Prashant Gupta − *Department of Mechanical Engineering and Materials Science, Institute of Materials Science and Engineering, Washington University in St. Louis, St. Louis, Missouri 63130, United States;* orcid.org/0009-0008-6291-9465

Yuwei Zhang − *Chemistry Department, Missouri University of Science and Technology, Rolla, Missouri 65409, United States*

Krishna Thapa − *Chemistry Department, Missouri University of Science and Technology, Rolla, Missouri 65409, United States*

Srikanth Singamaneni − *Department of Mechanical Engineering and Materials Science, Institute of Materials Science and Engineering, Washington University in St. Louis, St. Louis, Missouri 63130, United States;* orcid.org/0000-0002-7203-2613

Complete contact information is available at: https://pubs.acs.org/10.1021/acsaom.4c00086

Notes

The authors declare no competing financial interest.

ACKNOWLEDGMENTS

This work was supported by the National Science Foundation under grant CCF-1814797 and the Office of Research, Missouri University of Science and Technology.

REFERENCES

(1) Zhao, Y.; Xu, C. DNA-Based Plasmonic Heterogeneous Nanostructures: Building, Optical Responses, and Bioapplications. *Adv. Mater.* **2020**, *32* (41), e1907880.

(2) Zhou, H.; Yu, F.; Guo, C. F.; Wang, Z.; Lan, Y.; Wang, G.; Fang, Z.; Liu, Y.; Chen, S.; Sun, L.; Ren, Z. Well-oriented epitaxial gold nanotriangles and bowties on MoS2 for surface-enhanced Raman scattering. *Nanoscale* **2015**, *7* (20), 9153−7.

(3) Bhattarai, S. R.; Derry, P. J.; Aziz, K.; Singh, P. K.; Khoo, A. M.; Chadha, A. S.; Liopo, A.; Zubarev, E. R.; Krishnan, S. Gold nanotriangles: scale up and X-ray radiosensitization effects in mice. *Nanoscale* **2017**, *9* (16), 5085−5093.

(4) Soares, L.; Csaki, A.; Jatschka, J.; Fritzsche, W.; Flores, O.; Franco, R.; Pereira, E. Localized surface plasmon resonance (LSPR) biosensing using gold nanotriangles: detection of DNA hybridization events at room temperature. *Analyst* **2014**, *139* (19), 4964−73.

(5) Liebig, F.; Sarhan, R. M.; Bargheer, M.; Schmitt, C. N. Z.; Poghosyan, A. H.; Shahinyan, A. A.; Koetz, J. Spiked gold nanotriangles: formation, characterization and applications in surface-enhanced Raman spectroscopy and plasmon-enhanced catalysis. *RSC Adv.* **2020**, *10* (14), 8152−8160.

(6) Xie, X.; Liao, J.; Shao, X.; Li, Q.; Lin, Y. The Effect of shape on Cellular Uptake of Gold Nanoparticles in the forms of Stars, Rods, and Triangles. *Sci. Rep* **2017**, *7* (1), 3827.

(7) Kuttner, C.; Mayer, M.; Dulle, M.; Moscoso, A.; Lopez-Romero, J. M.; Forster, S.; Fery, A.; Perez-Juste, J.; Contreras-Caceres, R. Seeded Growth Synthesis of Gold Nanotriangles: Size Control, SAXS Analysis, and SERS Performance. *ACS Appl. Mater. Interfaces* **2018**, *10* (13), 11152−11163.

(8) Choi, B. K.; Kim, J.; Luo, Z.; Kim, J.; Kim, J. H.; Hyeon, T.; Mehraeen, S.; Park, S.; Park, J. Shape Transformation Mechanism of Gold Nanoplates. *ACS Nano* **2023**, *17* (3), 2007−2018.

(9) Kabusure, K. M.; Piskunen, P.; Yang, J.; Kataja, M.; Chacha, M.; Ojasalo, S.; Shen, B.; Hakala, T. K.; Linko, V. Optical characterization of DNA origami-shaped silver nanoparticles created through biotemplated lithography. *Nanoscale* **2022**, *14* (27), 9648−9654.

(10) Huang, Y.; Ferhan, A. R.; Gao, Y.; Dandapat, A.; Kim, D. H. High-yield synthesis of triangular gold nanoplates with improved shape uniformity, tunable edge length and thickness. *Nanoscale* **2014**, *6* (12), 6496−500.

(11) Heuer-Jungemann, A.; Linko, V. Engineering inorganic materails with DNA nanostructures. *ACS Cent. Sci.* **2021**, *7*, 1969−1979.

(12) Sun, W.; Boulais, E.; Hakobyan, Y.; Wang, W.; Guan, A.; Bathe, M.; Yin, P. Casting inorganic structures with DNA molds. *Science* **2014**, *346*, 1258361−8.

(13) Szustakiewicz, P.; Gonzalez-Rubio, G.; Scarabelli, L.; Lewandowski, W. Robust Synthesis of Gold Nanotriangles and their Self-Assembly into Vertical Arrays. *ChemistryOpen* **2019**, *8* (6), 705−711.

(14) Haes, A. J.; Zhao, J.; Zou, S.; Own, C. S.; Marks, L. D.; Schatz, G. C.; Van Duyne, R. P. Solution-phase, triangular ag nanotriangles fabricated by nanosphere lithography. *J. Phys. Chem. B* **2005**, *109* (22), 11158−62.

(15) Kim, J.; Song, X.; Ji, F.; Luo, B.; Ice, N. F.; Liu, Q.; Zhang, Q.; Chen, Q. Polymorphic Assembly from Beveled Gold Triangular Nanoprisms. *Nano Lett.* **2017**, *17* (5), 3270−3275.

(16) Wang, G.; Akiyama, Y.; Takarada, T.; Maeda, M. Rapid Non-Crosslinking Aggregation of DNA-Functionalized Gold Nanorods and Nanotriangles for Colorimetric Single-Nucleotide Discrimination. *Chemistry* **2016**, *22* (1), 258−63.

(17) Tan, S. F.; Anand, U.; Mirsaidov, U. Interactions and Attachment Pathways between Functionalized Gold Nanorods. *ACS Nano* **2017**, *11* (2), 1633−1640.

(18) Wang, G.; Zhang, Y.; Liang, X.; Takarada, T.; Maeda, M. Regioselective DNA Modification and Directed Self-Assembly of Triangular Gold Nanoplates. *Nanomaterials (Basel)* **2019**, *9*, 581.

(19) Scarabelli, L.; Coronado-Puchau, M.; Giner-Casares, J. J.; Langer, J.; Liz-Marzan, L. M. Monodisperse gold nanotriangles: size control, large-scale self-assembly, and performance in surface-enhanced Raman scattering. *ACS Nano* **2014**, *8* (6), 5833−42.

(20) Luo, B.; Kim, A.; Smith, J. W.; Ou, Z.; Wu, Z.; Kim, J.; Chen, Q. Hierarchical self-assembly of 3D lattices from polydisperse anisometric colloids. *Nat. Commun.* **2019**, *10* (1), 1815.

(21) Lechtman, E.; Pignol, J. P. Interplay between the gold nanoparticle sub-cellular localization, size, and the photon energy for radiosensitization. *Sci. Rep* **2017**, *7* (1), 13268.

(22) Liebig, F.; Sarhan, R. M.; Sander, M.; Koopman, W.; Schuetz, R.; Bargheer, M.; Koetz, J. Deposition of Gold Nanotriangles in Large Scale Close-Packed Monolayers for X-ray-Based Temperature Calibration and SERS Monitoring of Plasmon-Driven Catalytic Reactions. *ACS Appl. Mater. Interfaces* **2017**, *9* (23), 20247−20253.

(23) Ivaskovic, P.; Yamada, A.; Elezgaray, J.; Talaga, D.; Bonhommeau, S.; Blanchard-Desce, M.; Vallee, R. A. L.; Ravaine, S. Spectral dependence of plasmon-enhanced fluorescence in a hollow nanotriangle assembled by DNA origami: towards plasmon assisted energy transfer. *Nanoscale* **2018**, *10* (35), 16568−16573.

(24) Hung, A.; Micheel, C.; Bozano, L.; Osterbur, L.; Wallraff, G.; Cha, J. Large-area spatially ordred arrays of gold nanoparticles

directed by lithorgarphyically confined DNA origami. *Nat. Nanotechnol.* **2010**, *5*, 121−126.
(25) Shen, B.; Kostiainen, M. A.; Linko, V. DNA Origami Nanophotonics and Plasmonics at Interfaces. *Langmuir* **2018**, *34* (49), 14911−14920.
(26) Shen, C.; Lan, X.; Lu, X.; Meyer, T. A.; Ni, W.; Ke, Y.; Wang, Q. Site-Specific Surface Functionalization of Gold Nanorods Using DNA Origami Clamps. *J. Am. Chem. Soc.* **2016**, *138* (6), 1764−7.
(27) Liu, W.; Li, L.; Yang, S.; Gao, J.; Wang, R. Self-Assembly of Heterogeneously Shaped Nanoparticles into Plasmonic Metamolecules on DNA Origami. *Chemistry* **2017**, *23* (57), 14177−14181.
(28) Zhan, P.; Dutta, P. K.; Wang, P.; Song, G.; Dai, M.; Zhao, S. X.; Wang, Z. G.; Yin, P.; Zhang, W.; Ding, B.; Ke, Y. Reconfigurable Three-Dimensional Gold Nanorod Plasmonic Nanostructures Organized on DNA Origami Tripod. *ACS Nano* **2017**, *11* (2), 1172−1179.
(29) Chen, G.; Gibson, K. J.; Liu, D.; Rees, H. C.; Lee, J. H.; Xia, W.; Lin, R.; Xin, H. L.; Gang, O.; Weizmann, Y. Regioselective surface encoding of nanoparticles for programmable self-assembly. *Nat. Mater.* **2019**, *18* (2), 169−174.
(30) Zhan, P.; Wen, T.; Wang, Z. G.; He, Y.; Shi, J.; Wang, T.; Liu, X.; Lu, G.; Ding, B. DNA Origami Directed Assembly of Gold Bowtie Nanoantennas for Single-Molecule Surface-Enhanced Raman Scattering. *Angew. Chem., Int. Ed. Engl.* **2018**, *57* (11), 2846−2850.
(31) Li, N.; Shang, Y.; Han, Z.; Wang, T.; Wang, Z.; Ding, B. Fabrication of metal nanostructrues on DNA templates. *ACS Appl. Mater. Interfaces* **2019**, *11*, 13835−13852.
(32) Wang, J.; Fang, W.; Liu, H. Gold triangular nanoprisms: anisotropic plasmonic materials with unique structures and properties. *ChemPlusChem.* **2023**, *88*, e202200464.
(33) Yee, K. Numerical Solution of Initial Boundary Value Problems Involving Maxwell's Equations in Isotropic Media. *IEEE Trans. Antennas Propag.* **1966**, *14*, 302.
(34) Palik, E. *Handbook of Optical Constants of Solids*; Academic Press: Boston, MA, 1985.
(35) Reguera, J.; Langer, J.; de Aberasturi, D. J.; Liz-Marzán, L. M. Anisotropic metal nanoparticles for surface-enhanced Raman scattering. *Colloidal Synthesis of Plasmonic Nanometals* **2020**, 713−754.
(36) Park, J.-E.; Kim, J.; Nam, J.-M. Emerging plasmonic nanostructures for controlling and enhancing photoluminescence. *Chemical science* **2017**, *8* (7), 4696−4704.
(37) Kumar, A.; Kim, S.; Nam, J.-M. Plasmonically engineered nanoprobes for biomedical applications. *J. Am. Chem. Soc.* **2016**, *138* (44), 14509−14525.
(38) Johnson, P. B.; Christy, R. W. Optical constants of the noble metals. *Phys. Rev. B* **1972**, *6* (12), 4370.
(39) Dunn, K.; Elfick, A. Harnessing DNA nanotechnology and chemistry for application in photonics an electronics. *Bioconjugate Chem.* **2023**, *34*, 97−104.
(40) Arinze, E. S.; Qiu, B.; Nyirjesy, G.; Thon, S. M. Johnson, Plasmonic nanoparticle enhancement of solution-processed solar cells: practical limits and opportunities. *ACS Photonics* **2016**, *3*, 158−173.

https://doi.org/10.1021/acsaom.4c00086
ACS Appl. Opt. Mater. XXXX, XXX, XXX−XXX